Modeling and simulation of electrothermomechanical coupling phenomena in high power electronics

Peter Böhm, Y. C. Gerstenmaier, Ronald H. W. Hoppe, Yuri Iliash, George Mazurkevitch, Gerhard Wachutka

Angaben zur Veröffentlichung / Publication details:

Böhm, Peter, Y. C. Gerstenmaier, Ronald H. W. Hoppe, Yuri Iliash, George Mazurkevitch, and Gerhard Wachutka. 2002. "Modeling and simulation of electrothermomechanical coupling phenomena in high power electronics." *Lecture Notes in Computational Science and Engineering* 21: 393–400. https://doi.org/10.1007/978-3-642-55919-8_43.

Modeling and Simulation of Electrothermomechanical Coupling Phenomena in High Power Electronics

P. Böhm[1], Y.C. Gerstenmaier[1], R.H.W. Hoppe[2], Y. Iliash[2], G. Mazurkevitch[2], and G. Wachutka[1]

[1] Physics of Electrotechnology, Munich University of Technology, D-80290 Munich, Germany
[2] Institute of Mathematics , University of Augsburg, D-86159 Augsburg, Germany

Abstract. High power electronic devices based on innovative semiconductor technology play a significant role in technical applications. A robust operating behavior of such devices can be achieved by an optimal design taking into account the presence of coupled physical effects.
In this contribution, we focus on electrothermomechanical coupling phenomena in Integrated-High-Voltage Modules with housing and cooling mechanisms that are used as electric drives for high power electromotors. For the numerical solution of the underlying coupled systems of partial differential equations we consider efficient algorithmic tools such as domain decomposition techniques.

1 Introduction

The development and realization of innovative technologies for contact systems in high power electronics are currently subject of various activities both in basic research as well as in industrial practice. Particular interest is devoted to semiconductor based power devices as they are used in converter modules for energy transmission or as energy saving and low noise electric drives for high power electromotors in public transportation systems like trams or high speed trains. Significant aspects that have to be taken into account are reliability and safety of the used components. In order to guarantee a long term durability, the specific semiconductor devices have to be packed into appropriately designed modules that are integrated in housings filled with hard- and/or soft-cast.
Figure 1 displays a typical Integrated High-Voltage- (IHV-) module as developed by Siemens AG and eupec GmbH & Co KG (without the housing). In operational mode, the semiconductor devices produce Joule heat which results in a considerable self-heating of the entire module causing mechanical deformations due to heat stresses that can even lead to mechanical damage without appropriate cooling mechanisms. Therefore, the optimal design of the modules requires a subtle understanding of the electrothermomechanical coupling phenomena. This cannot be achieved by experimental means, since

during operation the most interesting parts in the module are not accessible to measurements. Therefore, efficient numerical simulation tools based on appropriate models have to be developed and implemented.

Concerning the applications oriented treatment of electrothermomechanical

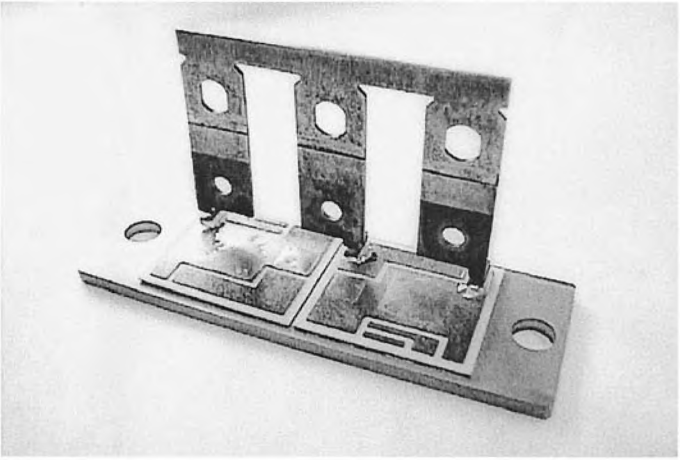

Fig. 1. IHV-module (without housing and semiconductor chips)

couplings in semiconductor device simulation, physically consistent and transparent models have been derived and validated on the basis of phenomenological thermodynamics [8,13–15], and numerical simulation techniques have been addressed in [3,7,9–12].

In this paper, suggested both by the discontinuous behavior of the material parameters across material interfaces and by the geometric structure of the module (cf. Fig. 2), we will use domain decomposition techniques on nonmatching grids also known as mortar element methods based on individual triangulations and discretizations of the subdomains and subdomain problems. This allows a great amount of flexibility at the expense of imposing weak continuity constraints across the interfaces to ensure consistency of the overall discretization (cf., e.g., [1,2,4–6,16]).

We discuss both the numerical solution of the resulting saddle point problems by multilevel block-preconditioned Lanczos iterations and adaptive grid refinement by efficient and reliable residual-type a posteriori error estimators. Numerical results are given illustrating the temperature distrubution, mechanical deformations, and stresses on selected clipping planes of real IHV-modules.

2 Electrothermomechanical Couplings in IHV-Modules

IHV-modules consist of specific semiconductor devices such as Insulated Gate Bipolar Transistors (IGBTs) and power diodes serving as switches for electric currents that are connected to the current contacts by wire bonds and integrated in copper housings (see Fig. 2). To prevent mechanical damage due to self-heating, the housings are mounted on several layers of different materials attached to each other by thin soldered joints. The copper ground plate is fixed on a cooling device (not explicitly shown in Fig. 2).

The operating behavior of the IGBTs and power diodes can be described by

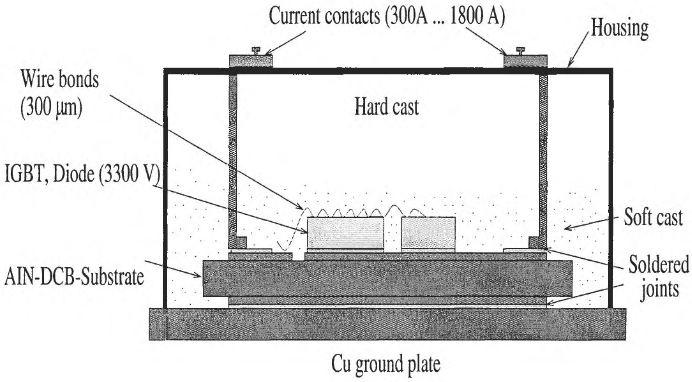

Fig. 2. Schematic representation of an IHV-module

the drift diffusion model (cf., e.g., [13–15]). Neglecting Thomson/Peltier and Nernst heat effects, the dominant heat source is the electric energy converted to Joule heat as given by $H_{Joule} := \mathbf{J}_n \cdot \mathbf{J}_n/(q\mu_n n) + \mathbf{J}_p \cdot \mathbf{J}_p/(q\mu_p p)$ where n and p are the carrier concentrations, $\mathbf{J}_n$ and $\mathbf{J}_p$ refer to the current densities, μ_n and μ_p stand for the mobilities, and q denotes the elementary charge.
The heat source is modelled by a heat flux $J(t)$ through the upper boundary Γ_0 of the module. At the lower boundary Γ_1 a heat exchange with the cooling device is assumed whereas the lateral boundary Γ_2 is supposed to be thermally insulated. Then, the temporal and spatial temperature distribution within the module is given by the following initial-boundary value problem

$$\rho c \frac{\partial T}{\partial t} = \nabla \cdot (\kappa \nabla T) \quad \text{in } Q := \Omega \times (t_0, t_1) \ , \tag{1}$$

$$\mathbf{n} \cdot \kappa \nabla T = J(t) \quad \text{on } \Gamma_0 \times (t_0, t_1) \ , \tag{2}$$

$$\mathbf{n} \cdot \kappa \nabla T = h\,(T^* - T) \quad \text{on } \Gamma_1 \times (t_0, t_1) \ , \tag{3}$$

$$\mathbf{n} \cdot \kappa \nabla T = 0 \quad \text{on } \Gamma_2 \times (t_0, t_1) \ , \tag{4}$$

$$T(x, t_0) = T_0(x) \quad \text{in } \Omega \ . \tag{5}$$

Here, the functions ρ, c and κ refer to the density, heat capacity, and thermal conductivity of the different materials. Moreover, h is the heat transition coefficient and T^* stands for the temperature of the ambient medium.
The self-heating of the module causes heat stresses leading to mechanical deformations $\mathbf{u}$ that can be described by the equilibrium equations

$$\mathrm{div}\,\sigma(\mathbf{u}) \;=\; \frac{\alpha(1-\nu)E}{(1+\nu)(1-2\nu)}\,\nabla(T-T_0) \quad \text{in } \Omega\subset\mathbf{R}^3 \;, \tag{6}$$

$$\mathbf{u} \;=\; \mathbf{0} \quad \text{on } \Gamma_0 \quad , \quad \mathbf{n}\cdot\sigma(\mathbf{u}) \;=\; \mathbf{0} \quad \text{elsewhere} \;. \tag{7}$$

where the stress tensor $\sigma(\mathbf{u})$ is related to the deformation rate tensor $\mathcal{D}(\mathbf{u}) := \frac{1}{2}(\nabla\mathbf{u}+(\nabla\mathbf{u})^T)$ by the constitutive equation

$$\sigma(\mathbf{u}) \;=\; \frac{E}{1+\nu}\;[\,\mathcal{D}(\mathbf{u}) \;+\; \frac{\nu}{1-2\nu}\;\mathrm{tr}\,\mathcal{D}(\mathbf{u})\,\mathbf{I}\,]\;.$$

Here, E and ν stand for Young's modulus and Poisson's ratio whereas α in (6) refers to the heat expansion coefficient.

3 Domain Decomposition Methods on Nonmatching Grids

The implicitly in time discretized heat equation (1)-(5) and the equilibrium equation (6),(7) give rise to boundary value problems for PDEs of the form $Lu = f$ with a second order elliptic differential operator L. Their weak formulations lead to variational problems

$$a(u,v) \;=\; \ell(v) \quad , \quad v\in V(\Omega)\;.$$

Here, $V(\Omega)\subset H^1(\Omega)$ resp. $V(\Omega)\subset(H^1(\Omega))^3$, $a: V(\Omega)\times V(\Omega)\to\mathbf{R}$ is a continuous $V(\Omega)$-elliptic bilinear form, and $\ell\in(V(\Omega))'$.
The computational domain $\Omega\subset\mathbf{R}^3$ is the bounded domain occupied by the IHV-module without housing. According to the sandwich-type structure of the module (cf. Fig. 2), we subdivide Ω into n mutually disjoint hexahedral subdomains $\bar\Omega := \bigcup_{i=1}^n \bar\Omega_i\,,\ \Omega_i\cap\Omega_j=\emptyset\,,\ 1\le i\ne j\le n$. We assume the partition to be geometrically conforming and refer to the union of the interfaces between adjacent subdomains $S := \bigcup_{i\ne j}\Gamma_{ij}\,,\ \Gamma_{ij} := \bar\Omega_i\cap\bar\Omega_j\,,\ |\,\Gamma_{ij}\,|>0$ as the skeleton of the decomposition.
We choose individual simplicial triangulations $\mathcal{T}_i$ of $\Omega_i\,,\ 1\le i\le n$, allowing nonconforming nodal points on the interfaces $\Gamma_{ij}\subset S$. We note that Γ_{ij} inherits a triangulation $\mathcal{T}_{ij}$ from $\mathcal{T}_i$ of Ω_i and a triangulation $\mathcal{T}_{ji}$ from $\mathcal{T}_j$ of Ω_j. We refer to Ω_j resp. Ω_i as the mortar resp. nonmortar side of Γ_{ij}.
The subdomain problems are discretized by continuous, piecewise linear finite elements. We denote by $V_h(\Omega_i;\mathcal{T}_i)$ the associated finite element spaces and consider the product space $V_h(\Omega) := \prod_{i=1}^n V_h(\Omega_i;\mathcal{T}_i)$. Clearly, functions

$v_h \in V_h(\Omega)$ may exhibit jumps $[v_h]_J$ across the interfaces $\Gamma_{ij} \subset S$. Therefore, in order to ensure consistency of the approach, we have to impose continuity constraints by means of appropriately chosen Lagrange multipliers which is done using the traces inherited from the nonmortar side. In particular, denoting by $S_{1,0}(\Gamma_{ij};\mathcal{T}_{ij})$ the finite element space of continuous, piecewise linear finite elements with respect to $\mathcal{T}_{ij}$ vanishing on $\partial\Gamma_{ij}$, we construct $M_h(\Gamma_{ij};\mathcal{T}_{ij})$ by a modification of those nodal basis functions in Γ_{ij} that have neighboring nodal points on $\partial\Gamma_{ij}$ such that $S_{1,0}(\Gamma_{ij};\mathcal{T}_{ij}) \subset M_h(\Gamma_{ij};\mathcal{T}_{ij})$ and $\dim M_h(\Gamma_{ij};\mathcal{T}_{ij}) = \dim S_{1,0}(\Gamma_{ij};\mathcal{T}_{ij})$ (for details see, e.g., [2]). The multiplier space is then given by $M_h(S) := \prod_{\Gamma_{ij}\subset S} M_h(\Gamma_{ij};\mathcal{T}_{ij})$, and weak continuity constraints are realized by the bilinear form $b_h : V_h(\Omega) \times M_h(S) \to \mathbf{R}$ with $b_h(v_h,\mu_h) := -\sum_{\Gamma_{ij}\subset S} \int_{\Gamma_{ij}} \mu_h [v_h]_J \, d\sigma$, $v_h \in V_h(\Omega)$, $\mu_h \in M_h(S)$. Moreover, setting $a_h : V_h(\Omega) \times V_h(\Omega) \to \mathbf{R}$ with $a_h(u_h,v_h) := \sum_{i=1}^{n} a_{\Omega_i}(u_h,v_h)$ where $a_{\Omega_i} := a \mid_{\Omega_i}$, the mortar finite element approximation is given by

$$a_h(u_h,v_h) \; + \; b_h(v_h,\lambda_h) = \ell(v_h) \quad , \quad v_h \in V_h(\Omega) \; , \tag{8}$$
$$b_h(u_h,\mu_h) \qquad\qquad = \quad 0 \quad , \quad \mu_h \in M_h(S) \; . \tag{9}$$

It can be shown that the bilinear form a_h is elliptic on the kernel of the operator associated with b_h and that b_h satisfies an LBB-condition (cf., e.g., [2]). In algebraic form the mortar element approximation (8),(9) gives rise to the saddle point problem

$$\begin{pmatrix} A & B^T \\ B & 0 \end{pmatrix} \begin{pmatrix} u \\ \lambda \end{pmatrix} = \begin{pmatrix} b \\ 0 \end{pmatrix} \tag{10}$$

where $A := \operatorname{diag}(A_1,...,A_n)$, $B^T := (B_1^T,...,B_n^T)^T$. For its numerical solution we use a preconditioned Lanczos-type iteration with a block-diagonal preconditioner of the form $\begin{pmatrix} R_u & 0 \\ 0 & R_\lambda \end{pmatrix}$. Here, $R_u := \operatorname{diag}(R_1,...,R_n)$ with subdomain preconditioners R_i being spectrally equivalent to the subdomain stiffness matrices A_i, $1 \le i \le n$, and R_λ represents an interface preconditioner being spectrally equivalent to the Schur complement $S_\lambda := B A^{-1} B^T$. We use multilevel preconditioners with respect to hierarchies of simplicial triangulations. In particular, the preconditioners R_i are chosen as the subdomain diagonal blocks of the BPX preconditioner. On the other hand, the construction of R_λ is realized by inner preconditioned Chebyshev iterations using a decomposition of S_λ into its subdomainwise counterparts and the construction of preconditioners for the corresponding subdomain Schur complements (for details we refer to [6]).

Grid adaptation is performed on the basis of an efficient and reliable residual-type a posteriori error estimator (cf. [4–6]). Assuming $h_i \le C\, h_j$ where $h_i := \{\operatorname{diam}(T) \mid T \in \mathcal{T}_i\,,\, T \cap \Gamma_{ij} \neq \emptyset\}$ and $h_j := \{\operatorname{diam}(T) \mid T \in \mathcal{T}_j\,,\, T \cap \Gamma_{ij} \neq \emptyset\}$, it can be shown that there exist constants $0 < \gamma_R \le \Gamma_R$ independent of the refinement level such that

$$\gamma_R\, \eta_R^2 \;\le\; \|u - u_M\|_{V(\Omega)}^2 \;\le\; \Gamma_R\, \eta_R^2$$

where in case the principal part of L is of the form $-\operatorname{div} a \operatorname{grad}$

$$\eta_R^2 := \sum_{i=1}^{n} \sum_{T \in \mathcal{T}_i} \eta_{R;T}^2 ,$$

$$\eta_{R;T}^2 := \underbrace{h_T^2 \, \|f - L\, u_M\|_{0;T}^2 + \sum_{F \subset \partial T \cap \Omega_i} h_F \, \|[\mathbf{n} \cdot a \, \nabla \, u_M]_J\|_{0;F}^2}_{\text{standard residual based error estimate w.r.t. } \mathcal{T}_i}$$

$$+ \underbrace{\sum_{F \subset T \cap S} h_F \, \|\mathbf{n} \cdot a \, \nabla \, u_M - \lambda_M\|_{0;F}^2 + \sum_{\ell=1}^{L} \sum_{F \subset \partial T \cap \Gamma_\ell} h_F^{-1} \, \|[u_M]_J\|_{0;F}^2}_{\text{additional part on the interfaces}} .$$

4 Numerical Results

For the design of IHV-modules one is interested in the distribution of the temperature T, the mechanical deformations $\mathbf{u}$, and the equivalence stresses $\sigma_E := \|\sigma^{(D)}\|_F$ where $\sigma^{(D)} := \sigma - \frac{1}{3}\,\mathrm{tr}\,(\sigma)\,\mathbf{I}$ is the deviatoric stress tensor and $\|\cdot\|_F$ refers to the Frobenius norm, i.e., $\|\sigma^{(D)}\|_F := (\sum_{i,j=1}^{3}(\sigma_{ij}^{(D)})^2)^{1/2}$. In particular, large equivalence stresses indicate possible mechanical failure. They are most likely to occur at the soldered joints. Figs. 3, 4, and 5 display the distribution of the computed values of $T, \mathbf{u}$, and σ_E in the clipping plane corresponding to the lower soldered joint between the copper ground plate and the copper plate above (cf. Fig. 2). We observe temperature peaks in the left and right part of the plane at locations just below the copper blocks housing the IGBTs and power diodes (Fig. 3). The mechanical deformations caused by the associated heat stresses are radially distributed towards the boundaries of the joint (Fig. 4). Moreover, we see that high equivalence stresses occur at the left and right lateral boundary of the joint which is in accordance with experimental findings.

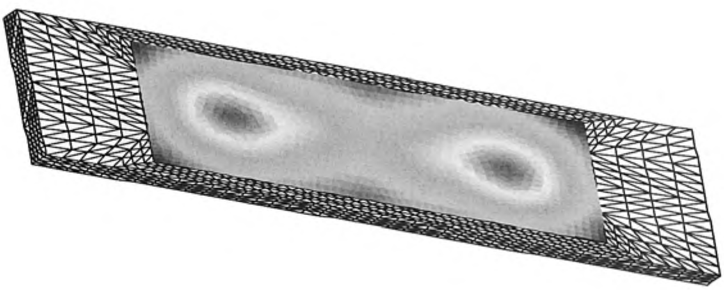

Fig. 3. Temperature distribution (cross section of lower soldered joint)

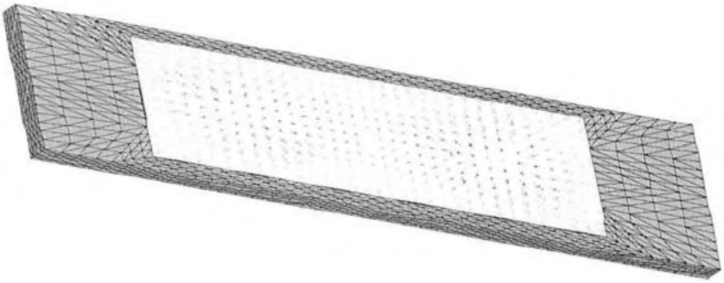

Fig. 4. Distribution of mechanical deformations (lower soldered joint)

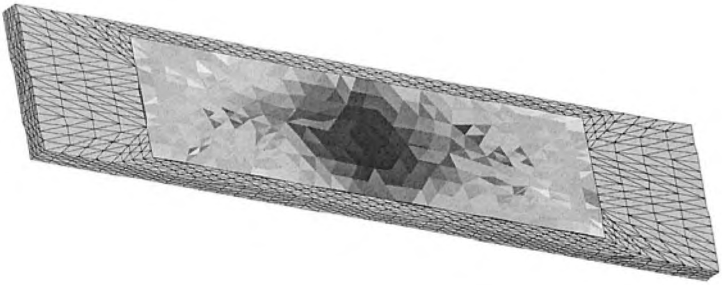

Fig. 5. Distribution of equivalence stresses (lower soldered joint)

Acknowledgments

The work has been supported by grants from the Federal Ministry for Education and Research (BMBF) under Grant No. 03HOM3A1 and from the German National Science Foundation (DFG) under Grant No. HO877/4-1.

References

1. F. Ben Belgacem and Y. Maday, "The mortar element method for three dimensional finite elements", RAIRO M^2AN **31**, 289-302, (1997).
2. D. Braess and W. Dahmen, "Stability estimates of the mortar finite element method for 3-dimensional problems", East-West J. Numer. Math. **6**, 249-263, (1998).
3. St. Dürndorfer, V. Gradinaru, R.H.W. Hoppe, E.-R. König, G. Schrag, and G. Wachutka, "Numerical simulation of microstructured semiconductor devices, transducers, and systems", In: High Performance Scientific and Engineering Computing. Proc. "Int. FORTWIHR-Symposium", Munich, March 1998 (H. Bungartz, F. Durst, and Chr. Zenger; eds.), pp. 309–323, Lecture Notes in Computational Science and Engineering, Vol. **8**, Springer, Berlin-Heidelberg-New York, (1999).
4. B. Engelmann, R.H.W. Hoppe, Y. Iliash, Y. Kuznetsov, Y. Vassilevski, and B. Wohlmuth, "Adaptive macro-hybrid finite element methods", In: Proc. 2nd European Conference on Numerical Methods (ENUMATH 97), Heidelberg, Sept.

29 - Oct. 3, 1997 (Bock,H.G.,Brezzi,F.,Glowinski,R.,Kanschat,G.Kuznetsov,Y., Périaux,J., and Rannacher,R.;eds.), p. 294-302, World Scientific, Singapore, (1998).

5. B.Engelmann, R.H.W.Hoppe, Y.Iliash, Y.Kuznetsov, Y.Vassilevski, and B. Wohlmuth, "Adaptive finite element methods for domain decomposition on nonmatching grids", In: "Parallel Solution of PDEs", IMA Volume in Mathematics and its Applications, Vol. 120 (P. Bjørstad and M. Luskin; eds.), pp. 57-83, Springer, Berlin-Heidelberg-New York, (2000).
6. R.H.W. Hoppe, Y. Iliash, Y. Kuznetsov, Y. Vassilevski, and B. Wohlmuth, "Analysis and parallel implementation of adaptive mortar element methods", East-West J. Numer. Math. **6**, 223-248, (1998).
7. R.H.W. Hoppe, Y. Iliash, and G. Mazurkevitch, "Domain decomposition methods in the design of high power electronic devices", In: "Multifield Problems. State of the Art" (M. Sändig, W. Schiehlen, and W. Wendland; eds.), pp. 169-182, Springer, Berlin-Heidelberg-New York, (2000).
8. K.D. Kells, "General electrothermal semiconductor device simulation", Hartung-Gorre, Konstanz, (1994).
9. K. Kells, K. Lilja, G. Wachutka, and W. Fichtner, "Detailed study of electrothermal effects in semiconductor power devices using multidimensional numerical simulation", In: Verhandlg. DPG(VI) **29**, HL-28.12, (1994).
10. K. Kells, S. Müller, W. Fichtner, and G. Wachutka, "Simulation of self-heating effects in a power p-i-n diode", In: Simulation of Semiconductor Devices and Processes (SISDEP-93), Vol. 5 (S. Selberherr, H. Stippel, and E. Strasser; eds.), p. 41-48, (1993).
11. S. Ramminger, G. Mitic, P. Türkes, and G. Wachutka, "Thermomechanical simulation of wire bonding joints in power modules", In: Proc. 2nd Conf. on Modeling and Simulation of Microsystems, Sensors, and Actuators (MSM-99), San Juan, Puerto Rico, pp. 483-486, (1999).
12. R. Thalhammer, G. Deboy, W. Keilitz, U. Müller, and G. Wachutka, "Electrothermal effects in semiconductor power devices analyzed by numerical simulation and internal laser deflection measurements", In: Proc. Int. Semiconductor Device Research Symp. (ISDRS-95), Charlottesville, U.S.A., pp. 51-54, (1995).
13. G.Wachutka, "Rigorous thermodynamic treatment of heat generation and conduction in semiconductor device modeling", IEEE Trans. CAD Integr. Circuits and Syst. **9**, 1141-1149, (1990).
14. G.Wachutka, "Problem-oriented modeling of coupled physical effects in microtransducers and electronic devices", In: Proc. 20th Int. Conf. on Microelectronics (MIEL-95), Nis, Serbia, Vol. 2, p. 539-547, (1995).
15. G. Wachutka, "The art of modeling coupled field effects in microdevices and microsystems", In: Proc. 2nd Int. Conf. on Modeling and Simulation of Microsystems, Sensors, and Actuators (MSM-99), San Juan, Puerto Rico, p. 14-19, (1999).
16. B. Wohlmuth, "Discretization Methods and Iterative Solvers Based on Domain Decomposition", Lecture Notes in Computational Science and Engineering, Vol. 17, Springer, Berlin-Heidelberg-New York, (2001).